

# Transport of TiO<sub>2</sub> nanoparticles through water saturated packed columns

V. Sygouni<sup>1\*</sup>, D. Vassilopoulos<sup>1</sup>, I.D. Manariotis<sup>1</sup> and C.V. Chrysikopoulos<sup>2</sup>

<sup>1</sup>Environmental Engineering Laboratory, Civil Engineering Department, University of Patras, 26504 Patras, Greece

<sup>2</sup>School of Environmental Engineering, Technical University of Crete, 73100 Chania, Greece

\*Corresponding author: E-mail: sygouni@upatras.gr, Tel +30 2610 996534, Fax: +30 2610 996573

## Abstract

In this work, various TiO<sub>2</sub> NP suspensions were prepared using different preparation techniques. Rutile-anatase and anatase TiO<sub>2</sub> NPs were used for the preparation of aquatic NP suspensions at various concentrations. Measurements of particles size and zeta potential were performed in order to investigate the effect of sonication and aging on nanoparticle agglomerates. Finally, transport experiments of TiO<sub>2</sub> NP solutions in packed columns were performed for varying TiO<sub>2</sub> concentrations. The concentration and size of the NPs were measured at the outlet of the column. It was observed that a substantial percentage of the NPs injected into the experimental column were retained in the column packing.

*Keywords: titanium oxides, nanoparticles, transport, particle size, porous media.*

## 1. INTRODUCTION

The application of engineered metal oxide nanoparticles (NPs), over the past few years, has considerably increased, especially in the areas of material science, cosmetics, and health industries. TiO<sub>2</sub> NPs are widely used in cosmetics, paints, catalysts and numerous other applications, and their potential uses are expected to increase further in the future [1]. Inevitably, NPs are discharged into wastewater and find their way to the aquatic and soil environment [2, 3]. The potential risks of NPs are dependent on their fate and transformations in the natural environment [3]. The investigation of interactions between nanoparticles and various solid surfaces found in the receiving environment is of crucial importance for improving our understanding of their fate and transport in environmental systems.

Nanomaterials have active surfaces, which are able to adsorb molecules in natural waters or molecules associated with other pollutants to be adsorbed. Recently, several studies have been conducted to investigate the surface charge, aggregation, and surface adsorption behaviour of TiO<sub>2</sub> NPs in a variety of conditions in order to better understand the fate of TiO<sub>2</sub> NPs in the environment [4, 5, 6]. It has been reported in the literature that the solution pH, surface charge, inorganic salts, and organic matter significantly affect the stability of TiO<sub>2</sub> NPs in aqueous solutions [4-7].

The transport of NPs in porous media is mainly controlled by the NP characteristics, porous media type and structure, solution chemistry, flow velocity and biofilm formation [8-10]. Furthermore, a large quantity of numerous NPs is introduced in the aquatic environment from several point sources and non point sources due to accidental releases. However, the prevailing mechanisms of NPs transport in soil and groundwater are not yet clearly understood.

The aim of this work was to investigate the effect of TiO<sub>2</sub> NP preparation techniques on their characteristics. Rutile-anatase and anatase TiO<sub>2</sub> NPs were used to prepare aquatic NP suspensions at various concentrations. The particle size and zeta potential of TiO<sub>2</sub> suspensions were determined

after physical aging and/or sonication. Furthermore, transport experiments of TiO<sub>2</sub> NP suspensions were conducted in a packed column for various TiO<sub>2</sub> concentrations.

## 2. MATERIALS AND METHODS

The TiO<sub>2</sub> NP suspensions at various pH values were prepared using TiO<sub>2</sub> Anatase (Aldrich 637254-50G, size < 25 nm) and TiO<sub>2</sub> Anatase-Rutile (Aldrich, code size < 100 nm). Two different preparation methods were applied. In the first method (M1), the TiO<sub>2</sub> suspensions were prepared by dispersing TiO<sub>2</sub> NPs in deionized water and then adjusting the pH to the desired value. In the second method (M2), the pH of deionized water was adjusted to the desired value, and then NPs were added to the solution. For both methods, pH value was reduced using a solution of HCl 0.1 M, whereas it was increased using a NaOH 0.6 M. Flowthrough experiments were conducted in glass columns with diameter of 2.54 cm and length of 30 cm, packed with 2-mm diameter glass spheres. Each NP suspension was sonicated in an ultrasound bath (Elma, TI-H-5) for specific time (usually 30 min). Subsequently, the NP solution was pumped into the column with a peristaltic pump (Masterflex, Cole Parmer). After the end of each experiment the glass spheres were cleaned carefully following the procedures suggested by Bergendahl and Grasso (1999) [11].

The size and zeta potential of the NPs were measured using a zeta sizer (Nano ZS, Malvern, UK). The NP concentrations were measured by a fluorescence spectrophotometer (Cary Eclipse, Varian Australia PTY LTD, Australia) using a quartz cuvette (10 mm\*10 mm), and excitation/emission wavelength of 625 nm [5].

## 3. RESULTS AND DISCUSSION

### 3.1 Effect of preparation techniques on two different kinds of TiO<sub>2</sub> NPs of varying pH

The NPs used in this study were prepared by methods M1 and M2, and their particle sizes and zeta potentials were measured and listed in Table 1. It should be noted that the particle sizes were smaller for anatase than rutile-anatase TiO<sub>2</sub> NP solutions, independently of the preparation technique used. Also, the particle sizes of the anatase TiO<sub>2</sub> NP solutions were affected by the solution pH. The zeta potential values were negative for anatase solutions, and were not affected by the solution pH (see Fig. 2). In the case of anatase-rutile solutions, the particle size did not depend on the solution pH when solutions were prepared with the M1 technique (see Fig. 1). The particle size in anatase-rutile solutions decreased with increasing pH when the solutions were prepared using M2 (see Fig. 1). The zeta potential for anatase-rutile solutions decreased with increasing pH (see Fig 2). For anatase-rutile, the zeta potential was positive for low pH values, whereas for medium and high pH values the zeta potential was negative, and much lower than the corresponding values for anatase solutions (see Fig. 2). For the solutions prepared by using the M2 technique, the zeta potential for anatase-rutile solutions was negative for all pH values examined, and smaller than the corresponding values for anatase solutions (see Fig. 2).

**Table I:** Zeta potential and particle size measurements

NP	Preparation method	pH	Zeta potential (mV)	Particle size (nm)
TiO <sub>2</sub> anatase	M1, no sonication	2.7	-6.7	383
			-3.4	360.6
			-12.6	526.5
		7.5	-7.3	
			-2.7	
			-12.1	
		11.3	-5.7	309.0
			-10.6	210.0
			-9.4	237.7
		12	-7.5	606.0
-12.6	474.0			
-10.2	596.0			
TiO <sub>2</sub> anatase	M2, no sonication	4	-8.4	242.0
			-8.0	293.2
			-14.2	220.0
		6.3	-2.8	122.0
			-7.7	333.3
			-0.9	227.5
		7.4	-2.3	
			-2.7	
			-1.9	
		10.4	-8.2	260.0
-15.5	274.0			
-4.8	486.4			
TiO <sub>2</sub> anatase - rutile	M1, no sonication	2.9	5.2	142.0
			7.7	115.8
			7.9	89.6
		6.1	-23.3	790.0
			-22.4	860.0
			-24.1	587.0
		11.2	-36.3	164.0
			-41.3	285.5
			-41.5	407.0
TiO <sub>2</sub> anatase - rutile	M2, no sonication	4	-13.3	844.0
			-12.3	731.0
			-13.0	854.0
		5.8	-19.1	531.0
			-17.7	758.0
			-18.4	744.0
		9	-28.2	647.0
			-28.6	712.0
			-29.5	582.0
		10.9	-42.8	465.0
-44.4	558.0			
-45.4	568.7			
TiO <sub>2</sub> anatase - rutile	M2, 30 min sonication	4	-8.9	1019.0
			-10.1	955.0
			-10.3	1188.0
		5.8	-29.7	433.0
			-30.3	404.0
			-29.0	476.8
		10.9	-43.3	289.0
			-41.7	324.0
			-42.0	365.0
TiO <sub>2</sub> anatase - rutile	M2, 30 min sonication, 1 day aging	4	-13.2	615.0
			-12.2	712.0
			-10.7	1106.0
		5.8	-26.8	420.6
			-25.9	414.0
			-26.3	419.0
		10.9	-40.6	200.0
			-41.9	280.0
			-42.0	321.0

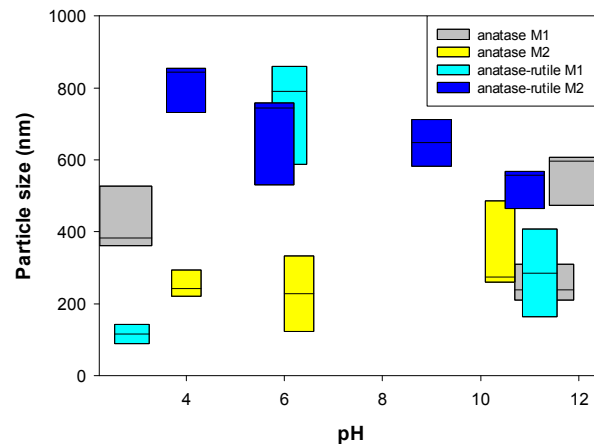


**Fig 1.** Particle size as a function of pH for 10 mg/L anatase and 10 mg/L anatase-rutile TiO<sub>2</sub> suspensions, prepared by M1 and M2 methods.

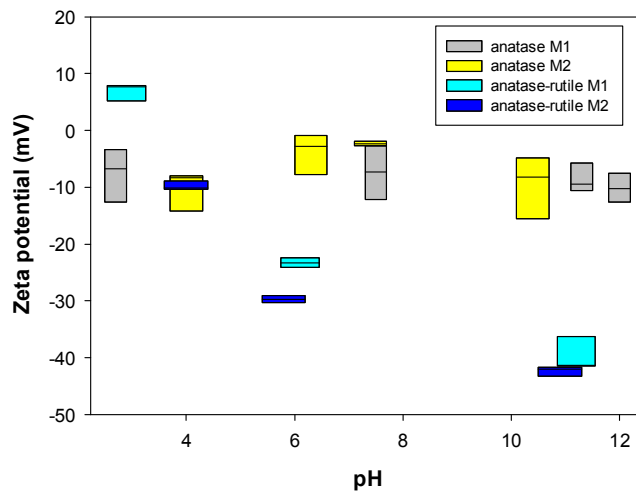


**Fig 2.** Zeta potential as a function of pH for 10 mg/L anatase and 10 mg/L anatase-rutile TiO<sub>2</sub> suspensions, prepared by the M1 and M2 methods.

The experimental results suggested that sonication of the NP suspension yielded a small range of particle sizes and zeta potential values (see Figs 3, 4) for all of the solutions prepared at medium pH values. At high pH values, the particle sizes remained unchanged following 1 day of aging.

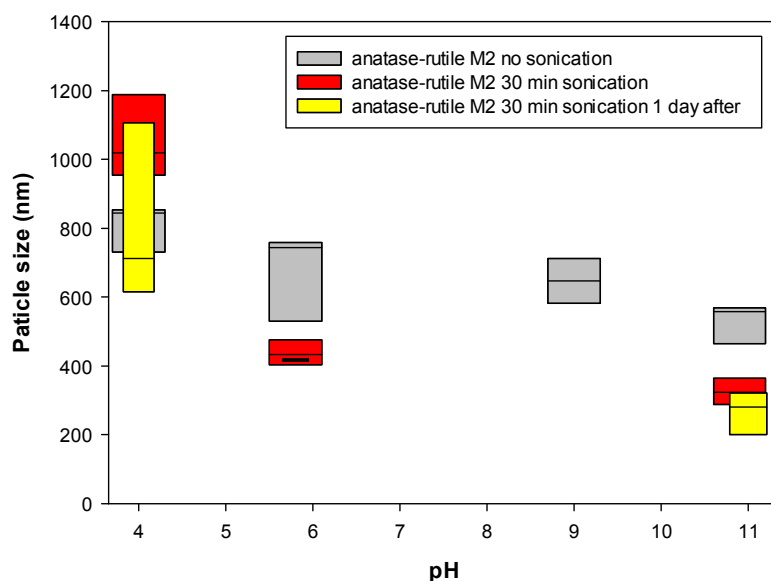


**Fig 3.** Particle size variation as a function of pH for 10 mg/L anatase-rutile TiO<sub>2</sub> suspensions, prepared by the M2 method.

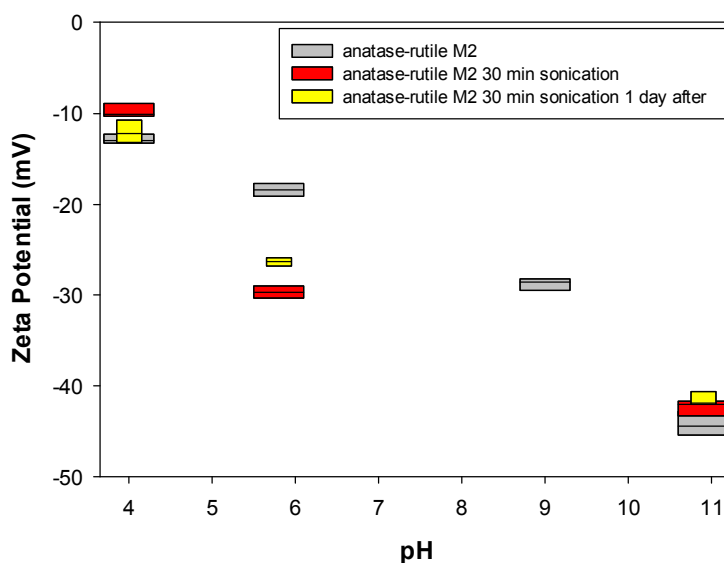


**Fig 4.** Zeta potential variation as a function of pH for 10 mg/L anatase-rutile TiO<sub>2</sub> solutions, prepared by the M2 method.

### 3.2 Transport of TiO<sub>2</sub> NPs through a packed column

The anatase TiO<sub>2</sub> suspensions were prepared at various concentrations using deionized water of pH=6.5 and they were continuously injected through a packed column. For each experiment, the injected TiO<sub>2</sub> suspension was replaced with deionized water as soon as the effluent TiO<sub>2</sub> concentration was stabilized. Effluent samples were collected periodically and analyzed for TiO<sub>2</sub> concentration and NP size. Two sets of experiments were conducted using the same flow rate: 2 mL/min for two different NP concentrations: 5 mg/L (see Figs 5, 6, 7), and 2.5 mg/L (see Figs 8, 9,

10). The normalized effluent particle concentration curves (see Figs 5 and 8) showed that the maximum (peak) concentration values were not the same for experiments with identical solution concentrations. This can be attributed to the fact that the particle sizes of the suspensions are not identical even for identical TiO<sub>2</sub> concentrations (see Figs 6, 9). Moreover, the effluent particle sizes during the experiments do not show a specific trend (see Figs 6, 9) suggesting that randomness plays an important role on the evolution of the experiments. However, the effluent concentration for every one of the experiments conducted was at the same level after the water injection. For the experiment with 5 mg/L TiO<sub>2</sub> solutions, the data from Experiment 3 exhibit the highest effluent concentration (see Fig. 5), and the particle sizes at the beginning of the experiment (t=0) in Experiment 3, are lower than those in Experiments 1 and 2 (see Fig. 6). Exactly the same behavior is observed for the experiment with 2.5 mg/L TiO<sub>2</sub> solutions (see Fig. 8). The maximum concentration for the three experiments conducted was not the same whereas in the case of Experiment 3 is higher (see Fig. 8) and the particle sizes were the smaller in the beginning of the experiment (see Fig. 9).

In order to extract some more information from the experimental data, the mass of TiO<sub>2</sub> accumulated in the column (M) is calculated using the following equation:

$$M_i = Q \left( \sum_{i=1}^{i_w} C_0 dt_i - \sum_{i=1}^{i_n} C_t dt_i \right) \quad (1)$$

and represents the difference between the effluent mass of TiO<sub>2</sub> and the mass injected through the column. Where,  $Q$  is the flow rate,  $i_w$  is the time interval where the water injection starts, and  $i_n$  is the time interval at the end of the experiment,  $C_0$  is the TiO<sub>2</sub> concentration at the inlet (which is constant for each experiment), and  $C_t$  is the effluent TiO<sub>2</sub> concentration at time t. The final percentage mass accumulation (FPM) is calculated using the ratio of the accumulated mass (M) to the mass injected through the column:

$$FPM = \frac{\left( \sum_{i=1}^{i_w} C_0 dt_i - \sum_{i=1}^{i_n} C_t dt_i \right)}{\sum_{i=1}^{i_w} C_0 dt_i} \quad (2)$$

In the case of flowthrough experiments with 5 mg/L TiO<sub>2</sub>, the accumulated mass for the Experiments 1 and 2, increases in the same rate and the final mass accumulation values are close whereas the initial particles sizes are very close for these two experiments (see Figs 6, 7). However, in the case of Experiment 3, the slopes of the curves in Fig. 7 show that the accumulation rate is smaller (see Figs 6, 7) than in the other two experiments, and the FPM is smaller, perhaps due to the smaller initial particle sizes and to the smaller forces which are developed between the particles. In the case of flowthrough experiments with 2.5 mg/L TiO<sub>2</sub>, the mass accumulation curves are almost identical for the three experiments with only difference in the peak values before water injection. The FPM is smaller for the Experiment 3, which is characterized by the smaller initial particle sizes (see Figs 9, 10). The normalized effluent concentration peaks for the flowthrough experiments of 5 mg/L varies between 0.15 to 0.45; whereas, for experiments of 2.5 mg/L varies between 0.1 and 0.18. Nevertheless, the peaks of the accumulated mass curves for the experiments of 5 mg/L are almost double than those of 2.5 mg/L (see Fig 11).

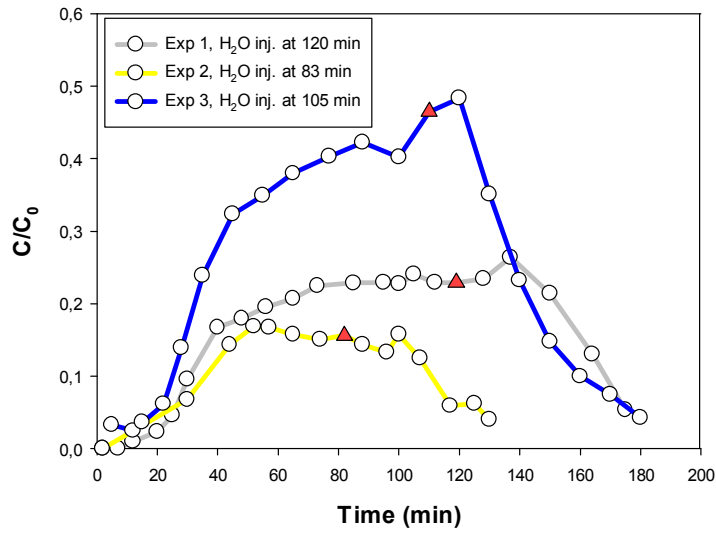


**Fig 5.** Normalized effluent  $\text{TiO}_2$  concentration versus time for initial concentration of 5 mg/L and flow rate of 2mL/min. Red points indicate the beginning of water injection.

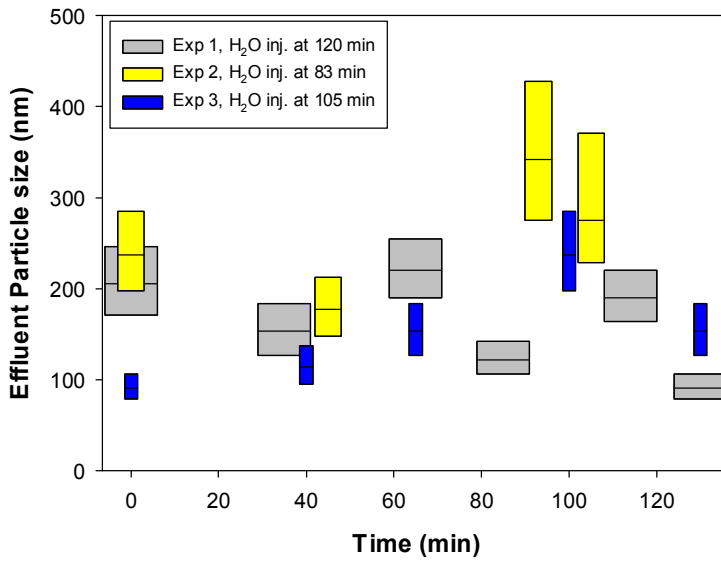


**Fig 6.** Observed effluent particle size from flowthrough experiments with 5 mg/L  $\text{TiO}_2$  and flow rate of 2 mL/min.

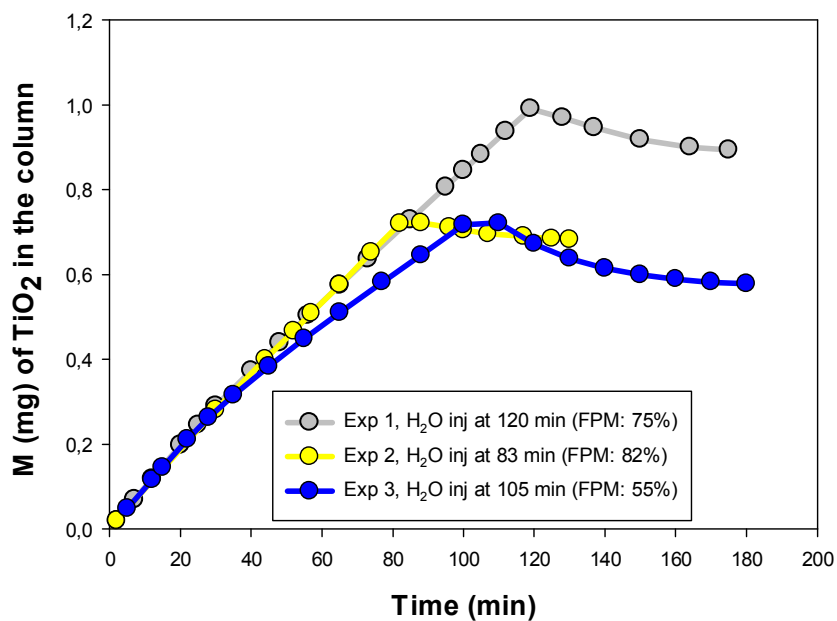


**Fig 7.** Accumulated mass of TiO<sub>2</sub> (M) calculated for flowthrough experiments with 5 mg/L TiO<sub>2</sub> and flow rate of 2 mL/min.

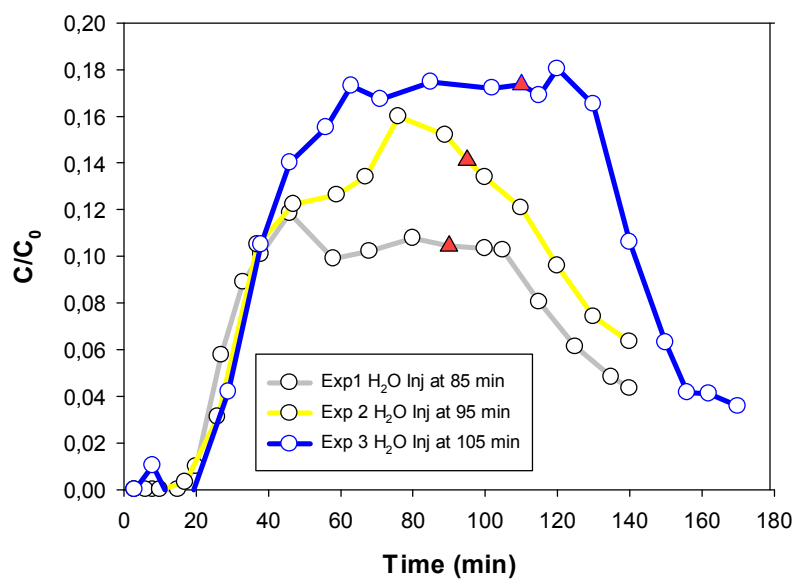


**Fig 8.** Normalized effluent TiO<sub>2</sub> concentration versus time for initial concentration of 2.5 mg/L and flow rate of 2 mL/min. Red points indicate the beginning of water injection



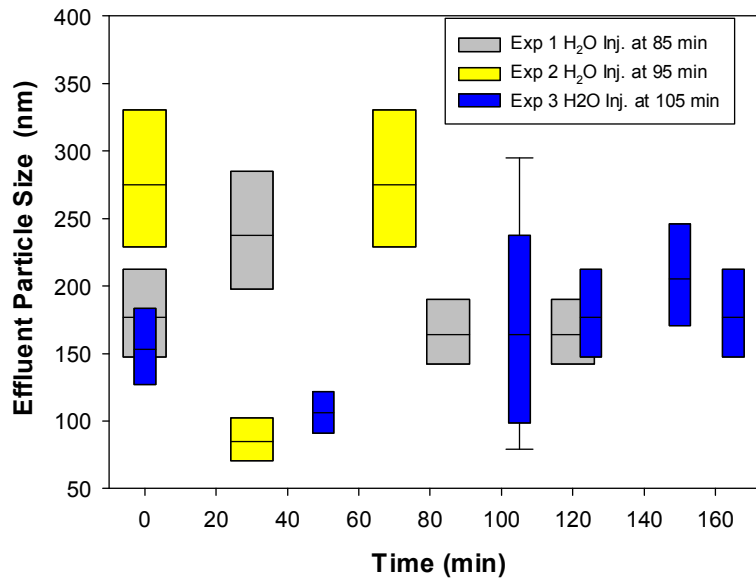


**Fig 9.** Observed effluent particle sizes from flowthrough experiments with 2.5 mg/L TiO<sub>2</sub> and flow rate of 2 mL/min.

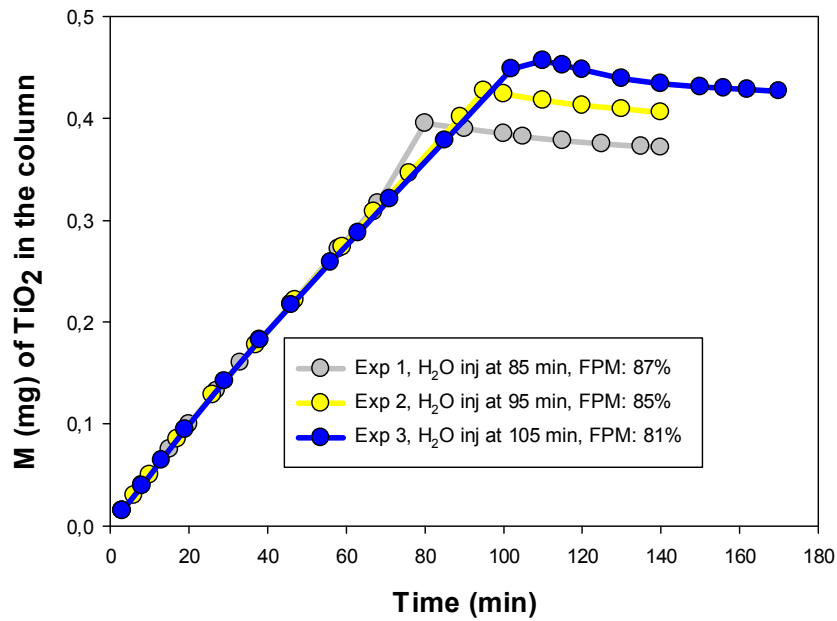


**Fig 10.** Accumulated mass of TiO<sub>2</sub> (M) calculated for flowthrough experiments with 2.5 mg/L TiO<sub>2</sub> and flow rate of 2 mL/min.

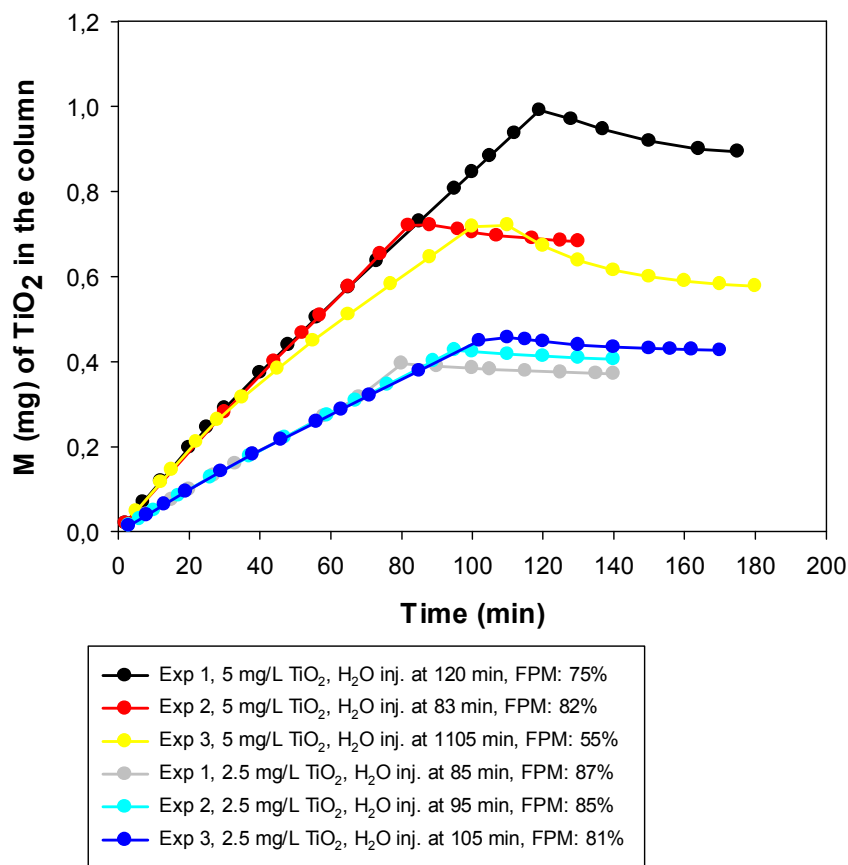


**Fig 11.** Accumulated mass of  $\text{TiO}_2$  (M) calculated for flowthrough experiments with 5 mg/L and 2.5 mg/L  $\text{TiO}_2$  and flow rate of 2 mL/min.

#### 4. CONCLUSIONS

- $\text{TiO}_2$  anatase suspensions are characterized by smaller aggregates than  $\text{TiO}_2$  anatase-rutile suspensions. Their sizes as well as the zeta potential of the suspensions were not affected by the solution pH. For anatase-rutile solutions the preparation technique plays an important role on aggregate size. The addition of anatase-rutile NPs in an aqueous solution with prefixed pH (M2) results in suspensions with aggregates of smaller size as the pH increases. Short-time sonication results in the decrease of particle sizes and zeta potential values at pH values close to neutral.
- Transport experiments of  $\text{TiO}_2$  anatase solutions through a column packed with glass beads showed that NP effluent concentration varied considerably, which can be attributed to the differences in the initial particles sizes. However the accumulated mass of  $\text{TiO}_2$  in the packed column do not diverge significantly for identical concentrations of  $\text{TiO}_2$  suspensions, when the initial particle size values are close.
- The initial particle size of suspensions play an important role on the evolution of mass accumulation concerning suspensions of identical concentrations. The FPM seems to be smaller for suspensions of smaller initial particle sizes.

## Acknowledgments

This research was partially funded by the European Union (European Social Fund-ESF) and Greek National Funds through the Operational program “Education and Lifelong Learning” under the action Aristeia I (Code No. 1185). This work is a collaboration between members of the Biomet network.

## References

1. Robichaud, C.O., Uyar, A.E., Darby, M.R., Zucker, L.G. and Wiesner, M.R. (2009). Estimates of upper bounds and trends in nano-TiO<sub>2</sub> production as a basis for exposure assessment. *Environmental Science and Technology*, **43**(12), 4227-4233.
2. Wiesner, M.R., Lowry, G.V., Alvarez, P., Dionysiou, D. and Biswas, P. (2006). Assessing the risks of manufactured nanomaterials. *Environmental Science and Technology*, **40**, 4336-4345.
3. Klaine, S.J., Alvarez, P.J.J., Batley, G.E., Fernandez, T.F., Handy, R.D., Lyon, D.Y., Mahendra, S., Mclaughlin, M.J. and Lead, J.R. (2008). Nanomaterials in the environment: behaviour, fate, bioavailability, and effects. *Environmental Toxicology and Chemistry*, **27**, 1825–1851.
4. Romanello, M.B. and Fidalgo de Cortalezzi, M.M. (2013). An experimental study on the aggregation of TiO<sub>2</sub> nanoparticles under environmentally relevant conditions. *Water Research*, **47**, 3887-3898.
5. Brunelli, A., Pojana, G., Callegaro, S., and Marcomini, A. (2013). Agglomeration and sedimentation of titanium dioxide nanoparticles (*n*-TiO<sub>2</sub>) in synthetic and real waters. *Journal of Nanoparticles Research*, **15**, 1684(1-10).
6. Xiang, C., Feng, Y., Li, M., Jaridi, M. and Wu, N. (2013). Experimental and statistical analysis of surface charge, aggregation and adsorption behaviors of surface-functionalized titanium dioxide nanoparticles in aquatic system. *Journal of Nanoparticles Research*, **15**, 1293(1-12).
7. Keller, A.A., Wang, H., Zhou, D., Lenihan, H.S., Cherr, G., Cardinale, B.J., Miller, R. and Ji, Z. (2010). Stability and aggregation of metal oxide nanoparticles in natural aqueous matrices. *Environmental Science and Technology*, **44**, 1962-1967.
8. Fang, J., Shan, X-Q., Wen, B., Lin, J-M., Owens, G. (2009). Stability of titania nanoparticles in soil suspensions and transport in saturated homogeneous soil columns. *Environmental Pollution*, **157**, 1101-1109.
9. Rottman, J., Sierra-Alvarez, R. and Shadman, F. (2013). Real-time monitoring of nanoparticle retention in porous media. *Environmental Chemistry Letters*, **11**, 71-76.
10. Jiang, X., Wang, X., Tong, M. and Kim, H. (2013). Initial transport and retention behaviors of ZnO nanoparticles in quartz sand porous media coated with *Escherichia coli* biofilm. *Environmental Pollution*, **174**, 38-49.
11. Bergendahl, J. and D. Grasso, (1999). Prediction of Colloid Detachment in a Model Porous Media: Thermodynamics. *Particle Technology and Fluidization AIChE J*, **45**, 475-484.